Anti-Jamming and Time Delay Performance Analysis of Future SATURN Upgraded Military Aerial Communication Tactical Systems

Taeho Yang*, Kwangyull Lee, Chulhee Han, Kyeongsoo An, Indong Jang, and Seungbeom Ahn
Hanwha Systems Co., Ltd. Seoul, South Korea
[e-mail: ted.yang@hanwha.com, ky0208.lee@hanwha.com, chulhee.han@hanwha.com, kyeongsoo.an@hanwha.com, indong.jang@hanwha.com, seungbeom.ahn@hanwha.com]
*Corresponding author: Taeho Yang

Received November 17, 2021; revised March 14, 2022; accepted May 5, 2022; published September 30, 2022

Abstract

For over half a century, the United States (US) and its coalition military aircrafts have been using Ultra High Frequency (UHF) band analog modulation (AM) radios in ground-to-air communication and short-range air-to-air communications. Evolving from this, since 2007, the US military and the North Atlantic Treaty Organization (NATO) adopted HAVE QUICK to be used by almost all aircrafts, because it had been revealed that intercepting and jamming of former aircraft communication signals was possible, which placed a serious threat to defense systems. The second-generation Anti-jam Tactical UHF Radio for NATO (SATURN) was developed to replace HAVE QUICK systems by 2023. The NATO Standardization Agreement (STANAG) 4372 is a classified document that defines the SATURN technical and operational specifications. In preparation of this future upgrade to SATURN systems, in this paper, the SATURN technical and operational specifications are reviewed, and the network synchronization, frequency hopping, and communication setup parameters that are controlled by the Network (NET) Time, Time Of Day (TOD), Word Of Day (WOD), and Multiple Word of Day (MWOD) are described in addition to SATURN Edition 3 (ED3) and future Edition 4 (ED4) basic features. In addition, an anti-jamming performance analysis (in reference to partial band jamming and pulse jamming) and the time delay queueing model analysis are conducted based on a SATURN transmitter and receiver assumed model.

Keywords: Anti-jamming, HAVE QUICK, time delay, SATURN.

http://doi.org/10.3837/tiis.2022.09.011 **ISSN : 1976-7277**

1. Introduction

After World War II, Ultra High Frequency (UHF) band AM radios that operate in the 225~400 MHz frequency range were used for ground-to-air communication and short-range air-to-air by the United States (US) and its coalition military aircrafts [1].

The US military and the North Atlantic Treaty Organization (NATO) adopted HAVE QUICK to be used by almost all aircrafts since 2007. The US military adopted HAVE QUICK in the 1980s because it was revealed that intercepting and jamming of an aircraft communication signal was very easy to do and could be conducted with relatively inexpensive and easily accessible electronic parts [2].

To avoid interception and jamming, a frequency hopping technology developed in the US was chosen to be used, where the system's codename was called HAVE QUICK. The HAVE QUICK airborne radio communications (ARC) system ARC-204 was used on the E-3 Sentry. The ARC-204 requires line-of-sight (LoS) when conducting ground operations, which made it suitable for use on the E-3 Sentry as it maintains LoS for very long distances during ground operations. HAVE QUICK uses Amplitude Modulation (AM) for voice signal modulation and Amplitude Shift Keying (ASK) for data modulation. In addition, the frequency hopping technology used in HAVE QUICK is not a digital signal encryption technology, but rather a physical UHF signal frequency switching scheme that changes its signal frequency based on the frequency hopping pattern. Since the signal frequency is rapidly changed, even if an enemy was eavesdropping on a certain frequency signal channel, only a small segment of the signal would be detected. In addition, due to the frequency hopping pattern, even if jamming of a selected channel frequency was conducted, total signal loss could be avoided [2].

The current HAVE QUICK system had improvements included and evolved in to the AN/ARC-164 HAVE QUICK II radio. NATO and the US military currently use the HAVE QUICK II radio in air-to-air, air-to-ground, and ground-to-air communications.

For example, the Aviation Units, Air Traffic Services and Ranger Units of the U.S. Army use HAVE QUICK II radios. In addition, tactical air operations of the US Air Force (USAF), US Navy (USN), and NATO use the UHF-AM mode of HAVE QUICK II radio for tactical communications [3].

However, as use of frequency hopping patterns have become more common and the new artificial intelligence (AI) signal analyzers can find frequency hopping patterns, additional signal protection became necessary. Therefore, the upgraded version of HAVE QUICK was developed [4].

The Second-generation Anti-jamming Tactical UHF Radio for NATO (SATURN) was developed to replace the HAVE QUICK systems by 2023. NATO and the US military will use SATURN for their tactical airborne operations, where the NATO Standardization Agreement (STANAG) 4372 is a classified document that defines the SATURN technical and operational specifications [4].

SATURN uses the digital modulation technology Minimum Shift Keying (MSK) for voice and data communication. MSK is a variant of the Frequency Shift Keying (FSK) digital modulation scheme, which can integrate frequency hopping in the most ideal way. The digital encryption technologies applied in SATURN significantly enhance the protection of the digital voice and data transferred over SATURN UHF radios [4].

This paper focuses on the upgradable systems that need to be implemented in preparation of the system integration of SATURN technology, which will replace HAVE QUICK and HAVE QUICK II systems by 2023. The following chapters of this paper are organized as follows. In chapter 2, HAVE QUICK, HAVE QUICK II, and SATURN control scheme is

introduced. In chapter 3, an anti-jamming performance analysis is conducted based on the SATURN transmitter and receiver assumed model. In chapter 4, a queueing performance analysis is conducted based on the SATURN transmitter and receiver assumed model, which is followed by the conclusion of this paper presented in chapter 5.

2. HAVE QUICK, HAVE QUICK II, and SATURN Control Scheme

HAVE QUICK, HAVE QUICK II, and SATURN use the same frequency range UHF band, which is from 225~400 MHz with a channel spacing of 25 kHz. However, HAVE QUICK uses AM for voice signal modulation and ASK for data modulation.

On the other hand, SATURN uses Minimum Shift Keying (MSK) for both voice and data communication. HAVE QUICK, HAVE QUICK II, and SATURN use waveforms that apply frequency hopping, however, HAVE QUICK and HAVE QUICK II use frequency hopping on analog modulated signals, and therefore, data loss occurs during tune times, which is the time period that the analog radio switches its signal's frequency channel.

Because SATURN uses frequency hopping on its digital MSK signals, all data and voice digitized signals are sent in digit forms, which makes SATURN signals lossless from burst outs between radio tune times and resilient enough to have anti jamming features. Full band and subband hopping nets with Plaintext and Ciphertext processing are used by HAVE QUICK, HAVE QUICK II, and SATURN.

The network synchronization, frequency hopping, and communication setup parameters are controlled by the Network (NET) Time, Time Of Day (TOD), Word Of Day (WOD), and Multiple Word of Day (MWOD), which are explained below [1].

2.1 WOD Control

HAVE QUICK, HAVE QUICK II, and SATURN all use WOD to control the frequency hopping rate and pattern [5]. Therefore, automatic setting of the WOD is critical to support the security level and jamming avoidance performance of HAVE QUICK, HAVE QUICK II, and SATURN systems.

In MWOD usage situations, the TOD and Day of the Month code are used together to specify what WOD should be used. HAVE QUICK, HAVE QUICK II, and SATURN systems automatically conduct WOD transitions to a new frequency hopping sequence at Greenwich Mean Time (GMT) based midnight time. This daily automatic change in WOD makes the frequency hopping sequence hard to predict by enemy systems. In addition, multiple WODs may use the tone time for programming the frequency hopping pattern and rate, where the maximum limit is set at 6. This presetting enables HAVE QUICK, HAVE QUICK II, and SATURN systems to change to different frequency hopping sequences during the day without having to change the WOD [1].

2.2 TOD and NET Control

The specifications of SATURN are defined in the STANAG 4246 documents of NATO, which were published in January of 1987, but are protected as secret confidential documents.

The SATURN system uses a fast frequency hopping pattern for voice and data communications up to 16 kbits/s rates [1].

The frequency hopping pattern is determined by three parameters, which are the TOD, WOD, and NET. The WOD determines the frequency hopping rate based on a 6 number pattern. The TOD determines the frequency hopping instant of time. The NET defines the network identification (ID) number that multiple users can use to communicate over the same

network, which is based on a frequency table.

The TOD operations modes are summarized below.

- GPS-TOD: Global Positioning System (GPS) within the aircraft is used for the TOD
- Auto-TOD: An external transmitted GPS is used for the TOD (basic setting of 15 seconds)
- Self-start/emergency: After self-start (00:00:00.000000) the TOD is transferred to another system

Assuming that the WOD has the following formation of "***ABC.DEF***" the description of the segments are provided below [1][5]-[7].

First segment (corresponding to the ***ABC.D*** part):

- Chooses the Combat mode or Training mode.
- 300.0***EF*** is Training mode and the other options are Combat mode.

Second segment (corresponding to the ***EF*** part):

- The last two numbers determine the hop rate of the frequency hopping system.
- The last two number are used to set the Conference mode (00/50: usable, 25/75: unusable), there the Conference mode is the mode that information can be exchanged.

NET is the network ID that determines what frequency to use among the list of frequencies. Based on selection of Combat mode or Training mode, the NET ID changes [1][5]-[7].

For example, consider the form ***ABC.DEF*** as the NET ID.

- ***A*** is fixed
- ***BC.D*** is the actual network ID
  - Training mode uses 00.0~01.5
  - Combat mode uses all options
- ***EF***: Operation mode
  - 00: HAVE QUICK I
  - 25: HAVE QUICK II (Europe)
  - 50: HAVE QUICK II Non-NATO (Non Europe regions and used during combat)
  - 75: HAVE QUICK IIa is reserved (used by SATURN)

Some representative NET ID examples are listed below [1][5]-[7].

- A45.225: NET ID of 452, HAVE QUICK II in Europe
- A00.325: NET ID is 3, HAVE QUICK II Europe, could be used for Training mode
- A32.475: NET ID is 324, can be used for SATURN

2.3 SATURN ED3 to ED4 Evolution Process

The US military's SATURN program has plans to enhance its tactical Software Defined Radio (SDR) technologies to include more advanced functionalities by including more modernized tactical waveforms with higher throughput and reliability as well as more robust anti-jamming capabilities [4]. Currently, SATURN Edition 3 (ED3) is widely used by the U.S. military and NATO forces. The enhanced Edition 4 (ED4) of SATURN will soon be ratified and used by the US DoD and NATO allies, where ED4 will include more advanced cryptography technology and will mandatorily include most of the ED3 optional modes [4].

3. Anti-Jamming Performance Analysis

In this section, an anti-jamming performance analysis is conducted based on the SATURN transmitter and receiver assumed model [8]-[16]. The system block diagram is presented in **Fig. 1**. The SATURN assumed model includes an error control encoder followed by the interleaver. The interleaver can be used to provide transmission pattern mixing such that burst errors will be scattered to make the error control decoder more effective in erroneous bit correction. The transmission sequence is followed by the Ψ-ary digital signal modulator and the MSK modulator. Then the frequency hopping pattern is added to the modulated MSK signal based on the network synchronization, frequency hopping pseudo noise (PN) sequence generator, and communication setup parameters that are controlled by the NET Time, TOD, WOD, and MWOD, which have been explained in Chapter 2. The MSK frequency hopping signal is transmitted by the UHF radio frequency (RF) modem over the UHF frequency channel, which is received at a SATURN receiver, and the reverse process is conducted to obtain the output data. This communication processing sequence is presented in **Fig. 1**.

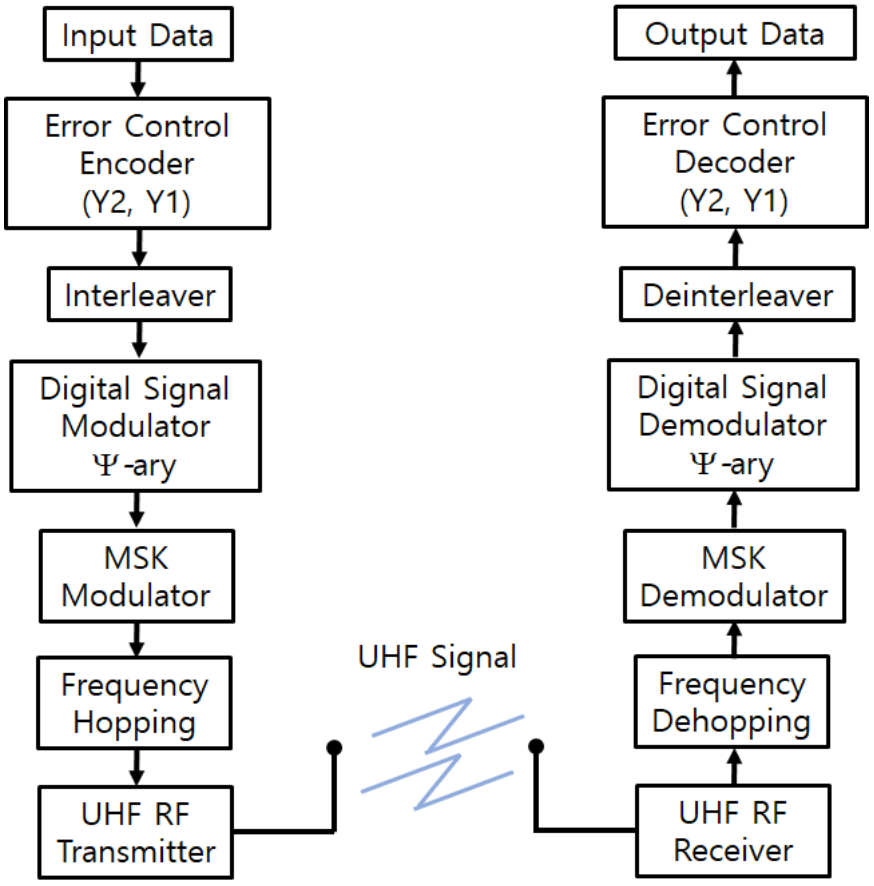

Fig. 1. SATURN transmitter and receiver assumed model.

In an Additive White Gaussian Noise (AWGN) environment using MSK, the chip error rate P_c can be expressed as in (1), where E_c is the average energy per chip, N_0 is the thermal noise at the receiver [8]-[16].

Table 1. SATURN assumed communication model specifications

Parameter	Value
Digital signal modulator CCSK code rate (X_1/X_2)	5/32
Error control encoder Reed-Solomon code rate (Y_2, Y_1)	(31, 15)
Nakagami fading channel density mean value (m)	2
Nakagami fading channel density standard deviation (σ)	1
Additive white gaussian noise (AWGN)	$10^{-14}, 10^{-12}$

In addition, a_c is defined as the received signal channel value, the Q represents the Q-function, $f(x)$ represents the Nakagami fading channel's probability density function (PDF), and $\Gamma(x)$ represents the gamma function. Based on these parameters, the MSK channel chip error rate can be expressed as in (1).

$$P_c = Q\left(\sqrt{\frac{2E_c}{N_0}}\right) \tag{1}$$

The effect of the code rate is included using E_c, where in the SATURN assumed model, the spreading code applied is cyclic code-shift keying (CCSK) that provides M-ary baseband modulation, where each symbol is presented by a chip sequence with code rate of r_c=5/32, and the channel coding for error control is a Reed-Solomon code with a code rate of r_s=15/31. Using the parameter information in **Table 1**, the channel chip error rate can be obtained from (2).

$$P_c = Q\left(\sqrt{\frac{\frac{2X_1Y_1}{X_2Y_2}E_b}{N_0}}\right) \tag{2}$$

For a more accurate performance analysis, the Nakagami fading channel density function is considered, which is presented in (3), which uses the parameter information in **Table 1** [8]-[16].

$$f_X(x^2) = \left(\frac{m}{\sigma^2}\right)^m \frac{x^{2(m-1)}}{\Gamma(m)} e^{-\left(\frac{m}{\sigma^2}\right)x^2} \tag{3}$$

The channel chip error rate without jamming while considering the Nakagami fading channel density function is presented in (4).

$$P_{c_0} = \int_0^\infty Q\left(\sqrt{\frac{\frac{2X_1Y_1}{X_2Y_2}a_c^2E_b}{N_0}}\right) f_{A_c}(a_c^2)da_c^2 \tag{4}$$

The channel chip error rate with jamming considered and the effects of the Nakagami fading included can be expressed as in (5).

$$P_{c_1} = \int_0^{\infty} \int_0^{\infty} Q\left(\sqrt{\frac{\frac{2X_1Y_1}{X_2Y_2}a_c^2 E_b}{N_0 + c_c^2 \frac{N_J}{\rho}}}\right) f_{A_c}(a_c^2) f_{c_c}(c_c^2) da_c^2 \, dc_c^2 \tag{5}$$

The symbol error rate in both cases (i.e., with jamming and without jamming) can be expressed using the equation below [8]-[16].

$$P_{s_i} \leq \sum_{j=0}^{32} \zeta_{UB\ j} \binom{32}{j} P_{c_i}^j \left(1 - P_{c_i}\right)^{32-j}, i = 0,1 \tag{6}$$

where $\zeta_{UB\ j}$ represents the upper bound of the symbol error rate according to the number of chip errors of the CCSK spreading code.

Based on the above equations, the average symbol error rate P_S for partial band jamming can be obtained from (7), where ρ_B represents the ratio of the bandwidth that is receiving a jamming attack divided by the overall SATURN communication signal bandwidth.

$$P_s = (1 - \rho_B) P_{s_0} + \rho_B P_{s_1} \tag{7}$$

The average chip error rate P_C for pulse jamming can be obtained from (8), where ρ_T represents the portion of time a transmitted symbol is under the influence of the pulse jamming signal.

$$P_c = (1 - \rho_T) P_{c_0} + \rho_T P_{c_1} \tag{8}$$

The average symbol error rate for pulse jamming can be obtained from (9) [8]-[16].

$$P_s \leq \sum_{j=0}^{32} \zeta_{UB\ j} \binom{32}{j} P_c^j (1 - P_c)^{32-j} \tag{9}$$

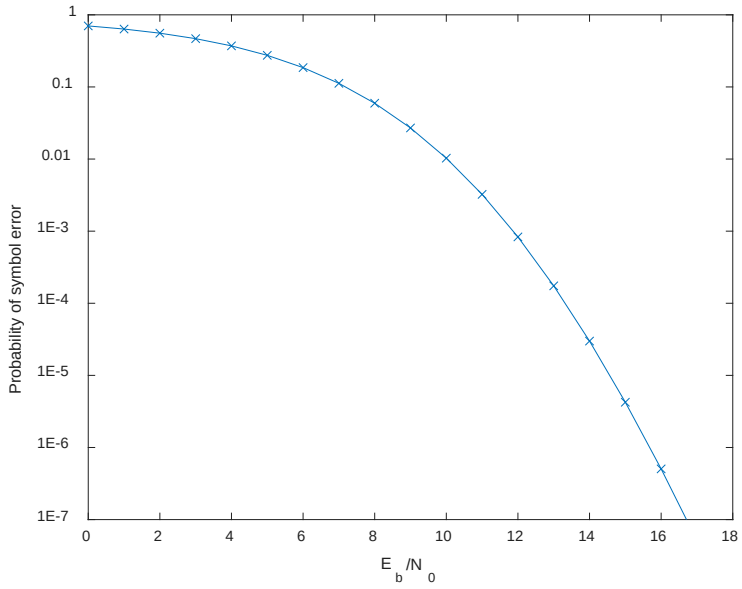

Fig. 2. Probability of symbol error without any jamming signal influence.

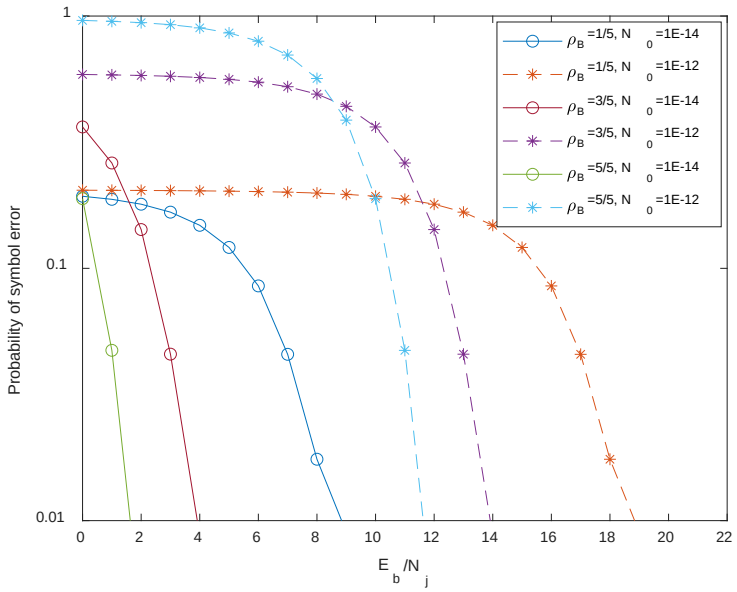

Fig. 3. Probability of symbol error based on partial band jamming (ρ_B) signal influence.

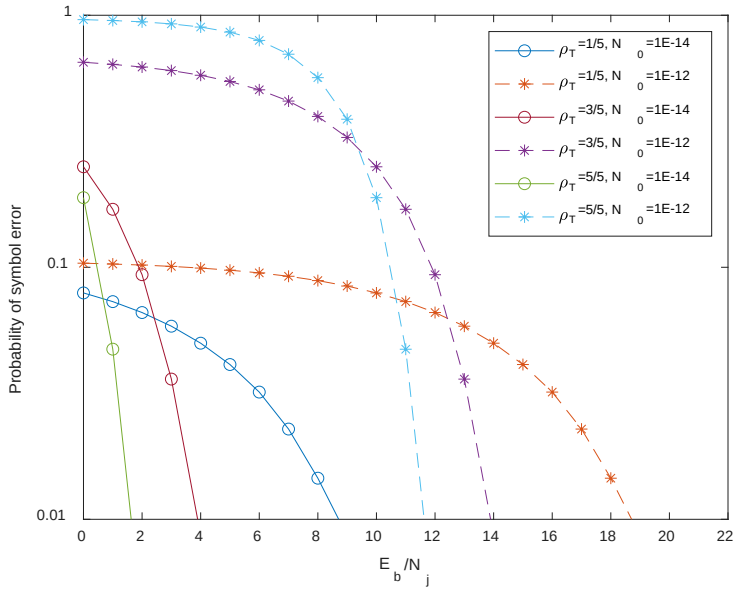

Fig. 4. Probability of symbol error based on pulse jamming (ρ_T) signal influence.

The probability of symbol error without any jamming signal influence is presented in **Fig. 2** [8]-[16]. The results of **Fig. 3** and **Fig. 4** show that partial band jamming is in general more detrimental to the communication performance when compared to pulse jamming [8]-[16]. In addition, it can be observed that as the ρ_B value in partial band jamming and the ρ_T in pulse jamming increase, the probability of symbol error increases significantly. Because the jamming signal is concentrated and the intensity of the jamming signal is strong for low ρ_B and ρ_T, the probability of symbol error does not change responsively even if the E_b/N_j values increase. For this reason, the probability of symbol error when ρ_B=ρ_T=5/5 with $N_0 = 10^{-14}$ is smaller than when ρ_B=ρ_T=3/5 with $N_0 = 10^{-14}$. Especially, under the worst condition of ρ_B=ρ_T=5/5 with $N_0 = 10^{-12}$, the probability of symbol error approaches 1 at low E_b/N_j values, where the only way to overcome this situation is to enhance the E_b/N_j level through more advanced transmission and adaptive filtering techniques.

4. Time Delay Performance Analysis

In this chapter, a queue based performance analysis is conducted based on the SATURN transmitter and receiver assumed model. The multiple queueing system is presented in **Fig. 5** [17]-[18].

For the multiple queueing system presented in **Fig. 5**, the server and queuing system mathematical parameters used in equations (10)~(15) and the parameter values applied in the simulation experiment are listed in **Table 2**.

In **Fig. 5**, each E_x system has its own queue and server, and messages from E_x are handled by the transmission scheduler. All messages are assumed to occur according to a Poisson distribution. To calculate the m_i response time, the queueing relations to $T_{E_i}^i$ and T_s^i need to be derived.

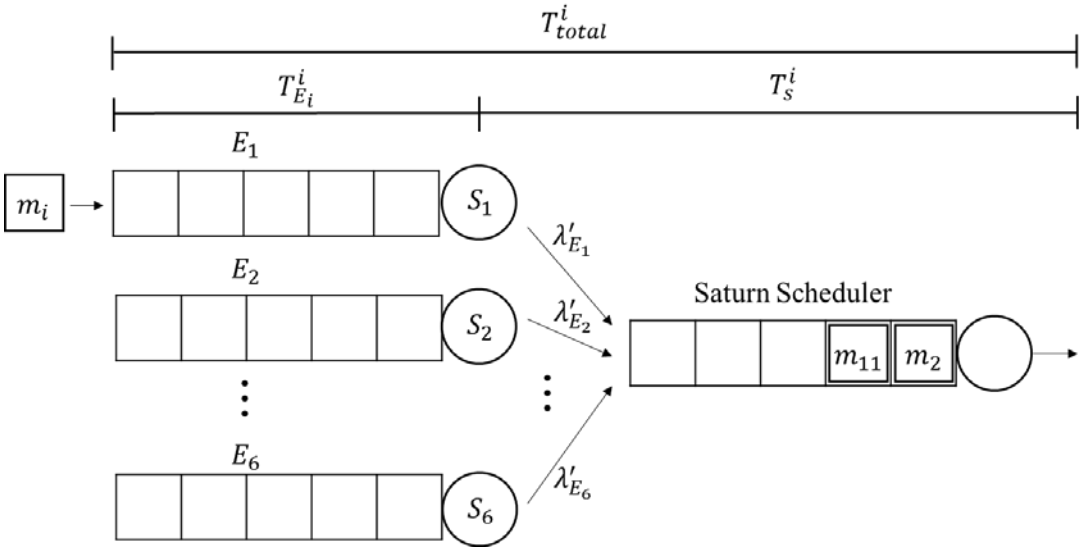

Fig. 5. Scheduling and queuing assumed model.

In the system, all messages are assumed to have a unique arrival rate and an E_x that occurs. The first step of the system model is to calculate the individual E_x queuing delay, where the equations are derived in (10)~(15). When a message occurs in E_x, it is stacked in the queue

and transmitted, and if there is a message that is being sent, it waits as long as the residual delay (10) before getting a chance to transmit it.

$$R_{E(x)} = \frac{1}{2}\lambda_{E(x)}\overline{X_{E_x}^2} \tag{10}$$

In the E_x system, the i^{th} message instance queueing delay can be calculated as follows. As shown in (11), it is calculated by the sum of queueing delay by other instance messages in the same E_x, which is E_i and self-delay. Self-delay refers to the time the same instance m_i occurs during additional waiting in the queue. Equation (12) provides $D_{E_i}^i$ which is the delay by other message instances m_k that belong to $E(i)$. Assuming that all messages occur according to the Poisson distribution, the delay is derived by the M/G/1 queuing formula [17]-[18]. Finally, the response time (13) that occurs in E_i is the sum of the transmission delay of m_i and $W_{E_i}^i$.

Table 2. Notation of assumed SATURN parameters

Variables	Description	Value
M	Message set of the system and the message instance is m_i	
$\lambda_{E_i}^i$	m_i arrival rate in E_i	Poisson (30)
λ_{E_x}	Average arrival rate for E_x	0.02-0.035
$u_{E_i}^i$	m_i service rate in E_i	5
$\overline{X_{E_i}^i} = \frac{1}{u_{E_i}^i}$	Average service (transmission) time of m_i in E_i	0.2
$\rho_{E_i}^i$	Network utilization of m_i in E_i	0.03-0.16
R_{E_x}	Residual time of E_x	< 0.004
$W_{E_i}^i$	Average queueing delay of m_i in E_i	< 0.4
$D_{E_i}^i$	Average queuing delay by other instances in the same $E_i$except m_i	< 0.45
$T_{E_i}^i$	Response time for E_i	0.2 ~ 0.62
d_i	Interarrival time for m_i	< 0.41
T_{total}^i	Total response time for m_i (system delay)	< 0.76
λ'_{E_x}	Average arrival rate of the path E_x and scheduler	< 0.05
λ_{all}	Total arrival rate of the system	< 2
μ_i	Service rate of m_i	5
$\bar{X} = \frac{1}{\mu_i}$	Average service of m_i	0.2
ρ_i	Network utilization for the entire system	< 0.36
R_i	Residual time	0.007 ~ 0.04
N_i	Average number of messages in the scheduler queue	0.03
W_Q^i	Average waiting time in the scheduler queue	< 0.15
T_s^i	System delay in the scheduler	< 0.35

$$W_{E_i}^i = \sum_{k\in E_i, k\neq i} D_{E_i}^k + \rho_{E_i}^i W_{E_i}^i \tag{11}$$

$$D_{E_i}^k = \rho_{E_i}^k W_{E_i}^k \tag{12}$$

$$T_{E_i}^i = R_{E_i} + W_{E_i}^i + \frac{1}{u_{E_i}^i} \tag{13}$$

To obtain response time after scheduling, the relationship between messages from different E_x must be considered, resulting in additional queueing delays. Messages entering the scheduler have as much delay, which is represented by (14) as the result of step 1 in their own interarrival time. The arrival rate of messages entering the scheduler queue from each E_x path is λ'_{E_x} and it is derived based on the average of $\frac{1}{d_i}$.

$$d_i = \frac{1}{\lambda^i_{E_i}} + T^i_{E_i} \tag{14}$$

Assuming that the number of E_x is 6 and λ_{all} is the total arrival rate in the system, which can be obtained from $\lambda_{all} = \sum_{x=1}^{6} \lambda'_{E_x}$. Each message that eventually enters the queue of the scheduler follows the Poisson distribution as periodic and non-periodic messages are mixed, and a delay by the step 1 process occurs. Therefore, it was modeled as a M/G/1 queueing system in this paper [17]-[18]. The response time of step 2 can be obtained by the sum of the residual delay (15), queueing delay (16), and transmission time of m_i, as presented in (17).

$$R = \frac{1}{2}\lambda_{all}\overline{X^2} \tag{15}$$

$$W^i_Q = \sum_{l \in M, l \notin E_i} \rho_l W^i_Q + \rho_i W^i_Q \tag{16}$$

$$T^i_s = R + W^i_Q + \frac{1}{\mu_i} \tag{17}$$

Finally, the response time of m_i is derived as (18).

$$T^i_{total} = T^i_{E_i} + T^i_s \tag{18}$$

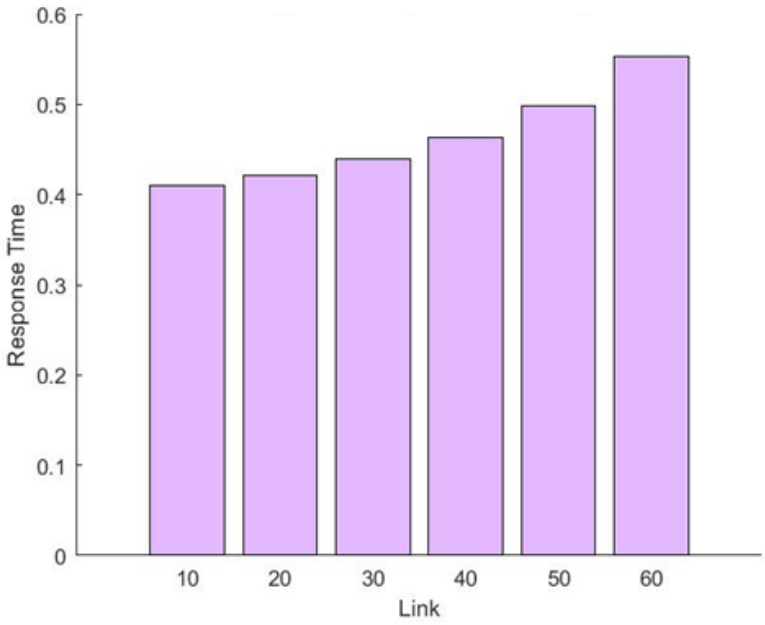

Fig. 6. Average link response time analysis.

Analytical model simulation for the average link response time is shown in **Fig. 6**. Analytical simulation was performed with 5 random seeds, which represents the average and variance values of all response times for each link case. When number of links are increased from 10 to 60, the average link response time correspondingly increased from 0.4098 to 0.5533, and the network utilization correspondingly increased from 0.05 to 0.36.

5. Conclusion

The transition to SATURN from the currently used HAVE QUICK II systems will be soon executed starting from 2023. This transition to SATURN will be conducted by the US military, NATO allies, and other countries that conduct joint operations and training with the US military. As the STANAG 4372 specifications are classified documents, this paper uses an assumed model for the SATURN performance analysis, which include an anti-jamming performance analysis and time delay queueing model analysis. The anti-jamming performance analysis was conducted based on the two models of partial band jamming and pulse jamming. In addition, the queueing system analysis uses M/G/1 models at the queues in the time delay analysis. The results reveal the parameters have a significant influence on the jamming and time delay performance, which can be used for advanced control in tactical operations of SATURN systems in the near future.

References

[1] T. Trpkosh, "SATURN, Comparison of SATURN and HAVEQUICK," Collins Aerospace, Cedar Rapids, Iowa, USA, Mar. 2019.
[2] L. Cloer, "8 Facts about HAVE QUICK Frequency Hopping System," *Repair and Engineering*, May 31, 2016.
[3] J. Pike and R. Sherman, "AN/ARC-164 HAVE QUICK II," FAS Military Analysis Network, Jan. 9, 1999,
[4] C. Barone, "Comparing the SATURN Waveform to HAVEQUICK and How it Improves Battlespace Comms," Ground Communication, May 9, 2019.
[5] "Solutions for Aviation," Overview 01.00, Rohde & Schwarz, Jun. 2019.
[6] "STANAG/MIL Waveforms Communicating on SDR Radios," Leonardo S.p.A., 2018.
[7] J. F. Keating, "A Cositable Ground Radio for Have Quick and Saturn," in *Proc. of IEEE Tactical Communications*, vol. 1, 1990. Article (CrossRef Link)
[8] H. Noh, J. Kim, J. Lim, J.-h. Nam, D.-w. Jang, "Anti-jamming Performance Analysis of Link-16 Waveform," *Journal of The Korean Institute of Communication Sciences*, vol. 35, no. 12, pp. 1105-1112, Dec. 2010.
[9] H. Wang, J. Kuang, Z. Wang, H. Xu, “Transmission performance evaluation of JTIDS,” in *Proc. of IEEE Military Communications Conference*, 2005. Article (CrossRef Link)
[10] C. Kao, C. Robertson, and K. Lin, “Performance analysis and simulation of cyclic code-shift keying,” in *Proc. of IEEE Military Communications Conference*, 2008. Article (CrossRef Link)
[11] R.A. Poisel, *Modern Communication Jamming Principles and Techniques*, Artech House, 2004.
[12] S. M. Rytov, Yu. A. Kravtsov, V. I. Tatarskii, *Principles of Statistical Radio physics 1*, Springer Verlag, 1987.
[13] M. Lichtman, R. P. Jover, M. Labib, R. Rao, V. Marojevic, and J. H. Reed, "LTE/LTE-A Jamming, Spoofing, and Sniffing: Threat Assessment and Mitigation," *IEEE Commun. Mag.*, vol. 54, no. 4, pp. 54-61, Apr. 2016. Article (CrossRef Link)

[14] B. R. Lee, E. K. Jung, S. Choe, "Link-16 Simulator Design over Jamming Environments and Time Synchronization Analysis," *Telecommunications Review*, vol. 23, no. 2, pp. 261-275, Apr. 2013.
[15] S. H. Aum, "SATURN Joint Tactical Radio System Interoperability with Link-22 and Link-16 Tactical Data Links," Ph.D. Dissertation, Department of Defense Fusion Engineering, Graduate School, Yonsei University, Aug. 2021.
[16] A. W. Lam and S. Tantaratana, "Theory and Applications of Spread-Spectrum Systems," *IEEE*, Pck Edition, Jun. 1994.
[17] D. Bertsekas & R. Gallager, *Data Networks*, 2nd Ed., NJ: Prentice Hall, 1992.
[18] W. Stallings, *High-Speed Networks and Internets: Performance & Quality of Service*, 2nd Ed., NJ: Prentice Hall, 2002.

Taeho Yang was appointed Head of Avionics and Space R&D department of Hanwha Systems in November 2020. Currently, he is leading Avionics and Satellite System teams to create value in the defense industry. After joining Samsung Electronics Co. and staying at the company during transition of its names to Samsung Thales and Hanwha Systems, he played major role in strengthening management of Hanwha System portfolios and placing Hanwha Systems as its leading defense company in Korea. Born in Seoul, he is a graduate of Hongik University majored in Electronics engineering and holds Master's degree of Electronics engineering from Kum-Oh Nat. Institute of Technology.

Kwangyull Lee was born in seoul, Korea, in 1962. He received the B.S. degrees in aeronautical engineering from Inha University, Incheon, Korea, in 1985. He joined the Samsung Precision company in 1985. From 2009 to 2015, he was the head of a PM3, the head of a sourcing group and Purchasing team leader at Samsung Thales. From 2015 to 2019, he was the head of the radar business team at Hanwha systems.
He was the leader of ISR Biz. Division. Currently, he is working at Hanwha Systems, Korea, as a Head of ISR Biz. His research interests include AESA, Radar, avionics systems, and small SAR satellite.

Chulhee Han received the B.S. degree in Electronic Engineering from Chung-ang University, Korea, in 1997, and M.S. and Ph.D. degrees in Electrical and Electronic Engineering from Yonsei University, Korea, in 1999 and 2007, respectively. Currently, he is working at Hanwha Systems, Korea, as a chief engineer. He was involved in various projects including tactical mobile WiMAX system, tactical LOS point-to-multipoint radio, and cognitive radio prototype. His research interests include Tactical Broadband Communications, Combat Network Radio, and Cognitive Radio for Military Applications.

Kyeongsoo An received the BS degree in electronic and electrical engineering from Busan National University and MS degree in electronic and electrical engineering from Kyungpook National University, in 2002 and 2009. After joining Samsung Thales Co. in 2002 and staying at the company during transition of its names to Hanwha Systems, he played major role in avionics R&D and designed lots of avionics computer and glass cockpit system. He was appointed Team leader of Avionics R&D Team of Hanwha Systems in 2018. His research interests include computer engineering, avionics systems, and airworthiness certification

Indong Jang received the BS degree in computer science and statistics from Daegu University, and the MS degree in computer engineering from Kyungpook National University, Republic of Korea, in 2002. From 2002 to 2007, he was a research engineer with the Electronics and Telecommunications Research Institute(ETRI). From 2007 to 2011, he was a senior research engineer with the Agency for Defense Development(ADD). Since 2011, he has been a chief engineer and is currently the Part Leader of Avionics System Team at Hanwha Systems. His research interests include computer engineering, avionics systems, and airworthiness certification.

Seungbeom Ahn was born in Gwangju, Korea, in 1978. He received the B.S., M.S and Ph.D. degrees in electronic and electrical engineering from Hongik University, Seoul, Korea, in 2004, 2006 and 2011, respectively. From 2011 to 2017, he was Senior Engineer with LS Electric. From 2017 to 2020, he was Senior Research Engineer with Korea Aerospace Industries. In May 2020, he is currently Chief Engineer with Hanwha Systems. His research interests include structure antenna analysis and design system integration of antennas and radios for aircraft, and test and evaluation for avionics.